ELSEVIER

FEMS Microbiology Letters 252 (2005) 299–307

FEMS MICROBIOLOGY Letters

www.fems-microbiology.org

Molecular cloning and functional analysis of (*R*)-3-hydroxyacyl-acyl carrier protein:coenzyme A transacylase from *Pseudomonas mendocina* LZ

Leo Zhong Zheng [1], Zhi Li [1], Hong-Lei Tian, Ming Li, Guo-Qiang Chen *

MOE laboratory of Protein Science, Department of Biological Sciences and Biotechnology, Tsinghua University, Beijing 100084, China

Received 26 May 2005; received in revised form 28 August 2005; accepted 6 September 2005

First published online 22 September 2005

Edited by A. Steinbuchel

Abstract

An inactive (*R*)-3-hydroxyacyl-acyl carrier protein:coenzyme A transacylase ($PhaG_{Pm}$) was cloned from a newly isolated Proteobacteria *Pseudomonas mendocina* LZ. It is the first characterized native inactive PhaG protein. Sequence analysis indicated that there were only two sites where the amino acid sequence differed between this inactive protein and the functional $PhaG_{Pp}$ from *P. putida*. The differences were located at position 78 and in the region 109–113 in the amino acid sequence. Mutagenesis was carried out to investigate these two sites. A recombinant strain harboring a S78C $PhaG_{Pp}$ mutant accumulated polyhydroxyalkanoates (PHA) at 11.9% of the cellular dry weight, as compared to the 21.6% PHA produced by the recombinant harboring the wild-type $PhaG_{Pp}$. On the other hand, the changes in the amino acid region 109–113 of $PhaG_{Pp}$ to its corresponding region of $PhaG_{Pm}$ resulted in negligible PHA accumulation. This demonstrated that region 109–113 in PhaG is relatively important for transacylase activity, while position 78 just plays a supporting role for the enzyme. Furthermore, 3-D structural models of $PhaG_{Pp}$ and $PhaG_{Pm}$ developed by computational prediction revealed that the variation in amino acids at 109–113 leads to the destruction of the PhaG catalytic center, resulting in the loss of enzyme activity.
© 2005 Federation of European Microbiological Societies. Published by Elsevier B.V. All rights reserved.

Keywords: PHB; Polyhydroxyalkanoates; (*R*)-3-Hydroxyacyl-acyl carrier protein:coenzyme A transacylase; PhaG; *Pseudomonas mendocina*

1. Introduction

Polyhydroxyalkanoates (PHA) are produced by various microorganisms as intracellular carbon and energy sinks under conditions of nutrient-imbalance [1–3]. More than 150 different PHA monomer structures have been identified, and PHA macromolecules have been classified into three sub-catalogues based on the monomer composition: short-chain-length (scl) PHA (C3–C5), medium-chain-length (mcl) PHA (C6–C14), and scl-mcl-copolymer PHA [1–3]. Recently, PHA are being considered as alternatives for petrochemical-based plastics because they are biodegradable thermoplastics [4]. PHA are also expected to become new tissue engineering materials due to their excellent biocompatibility properties [5–7].

The composition of PHA depends on the substrate specificity of PHA synthase, the carbon source supplied, and the precursor metabolic pathway involved [1–3]. Most *Pseudomonas* strains belong to the rRNA homology group I containing γ subdivision Proteobacteria,

* Corresponding author. Tel.: +86 10 62783844; fax: +86 10 62788784.

E-mail address: chengq@mail.tsinghua.edu.cn (G.-Q. Chen).

[1] Both authors contributed equally to this study.

0378-1097/$22.00 © 2005 Federation of European Microbiological Societies. Published by Elsevier B.V. All rights reserved.
doi:10.1016/j.femsle.2005.09.006

Downloaded from http://femsle.oxfordjournals.org/ by guest on January 23, 2016

such as *Pseudomonas putida* [8], *P. aeruginosa* [8], and *P. stutzeri* [9], are able to accumulate mcl-PHA from carbon sources unrelated to PHA structure by employing fatty acid de novo biosynthesis pathway [1–3,8]. Intermediates of this pathway, (*R*)-3-hydroxyacyl-acyl carrier proteins (ACPs) are converted to their corresponding coenzyme A (CoA) thioester derivatives to serve as the substrates of PHA synthase. The conversion can be mediated in a one-step reaction catalyzed by (*R*)-3-hydroxyacyl-ACP:CoA transacylase (PhaG), encoded by the *phaG* gene [10]. Thus, PhaG represents the key enzyme activity for mcl-PHA synthesis from unrelated carbon sources, such as carbohydrates. Interestingly, heterologous expression of *phaG* in non-PHA biosynthesis *Escherichia coli* strains could induce extracellular accumulation of 3-hydroxydecanoic acid [11], while thioesterase II plays an important assisting role in this process [12].

Recent studies have shown that the *phaG* gene exists in a broad range of bacterial species, including *P. putida* [10], *P. aeruginosa* [13], *P. oleovorans* [14], *Pseudomonas* sp. 61-3 [15], *P. stutzeri* [9], *P. nitroreducens* [9], and even non-*Pseudomonas* strains such as *Burkholderia caryophylli* which belongs to the rRNA homology group II β subdivision Proteobacteria [9], and pathogenic *Aeromonas hydrophylla* which is a member of Aeromonadaceae (formerly Vibrionaceae, unpublished result). However, additional details concerning this enzyme remain unclear. In this study, an inactive (*R*)-3-hydroxyacyl-ACP:CoA transacylase was cloned from a newly isolated strain *P. mendocina* LZ and, for the first time, the differences between this protein and the active PhaGs were studied.

2. Materials and methods

2.1. Bacterial strains, plasmids and culture conditions

Bacterial strains and plasmids used in this study are summarized in Table 1. *P. mendocina* LZ was isolated from oil-contaminated soil samples in northern China and identified by the Institute of Microbiology, Academic Sinica in Beijing, China. All strains were cultivated at 30 °C and 200 rpm overnight in Luria–Bertani (LB) medium [17]. 2.5 ml inocula from the overnight-cultured broth was added to fresh mineral salt (MS) medium containing the indicated carbon source and further incubated at 30 °C on a rotating shaker (NBS Series 25D, New Brunswick, USA) at 200 rpm for 48 h. MS medium contained per liter: 6.7 g $Na_2HPO_4 \cdot 7H_2O$, 1.5 g of KH_2PO_4, 0.5 g of $(NH_4)_2SO_4$, 0.2 g of $MgSO_4 \cdot 7H_2O$, 60 mg of ferrous ammonium citrate, 10 mg of $CaCl_2 \cdot 2H_2O$, and 1 ml of trace-element solution. Each liter of trace-element solution (pH 7.0) contained: 0.3 g H_3BO_3, 0.2 g $CoCl_2 \cdot 6H_2O$, 0.1 g $ZnSO_4 \cdot 7H_2O$, 0.03 g $MnCl_2 \cdot 4H_2O$, 0.03 g $NaMoO_4 \cdot 2H_2O$, 0.02 g $NiCl_2 \cdot 6H_2O$, and 0.01 g $CuSO_4 \cdot 5H_2O$. The carbon source was added at the beginning of the fermentation, and the pH was adjusted to 7.0. As necessary, 50 mg L^{-1} kanamycin was added to the medium to maintain the stability of the plasmids.

2.2. DNA manipulations

Ex Taq DNA polymerase was purchased form TaKaRa (Dalian, China); T4 DNA ligase and the pGEM®-T vector system I were purchased from Promega (Madison, WI, USA); restriction endonucleases were purchased from New England Biolabs (Beverly, MA, USA). All primers, as listed in Table 1, were supplied by BioAsia Co. (Shanghai, China). The conjugation technique was conducted as described by Simon et al. [16], in which *E. coli* S17-1 was employed as a donor strain. Mutagenesis was conducted employing the QuickChange®XL Site-Directed Mutagenesis Kit (Stratagene Co.). All other genetic techniques were performed following either standard procedures [17] or the manufacturers' instructions. DNA sequences of new plasmid constructs and mutations used in this study were confirmed by DNA sequencing by Shenergy Biocolor BioScience & Technology Co. Ltd. (Shanghai, China).

2.3. Cloning of the phaG gene and plasmid construction

A touchdown PCR employing primers NT and CT was applied to obtain the preferred product and minimize artifacts from pLZZGPp [11] and purified *P. mendocina* LZ genome. After an initial 2 min denaturation at 95 °C, the annealing temperature was shifted from 65 °C (5 cycles) to 60 °C (5 cycles) and then to 55 °C (25 cycles). Elongation was maintained at 72 °C for 2 min, with the last step for 5 min at 68 °C [9]. The resulting PCR products harboring *phaG* genes from *P. putida* and *P. mendocina* LZ were inserted into the vector pGEM-T (Promega, USA) for DNA sequencing. The PCR products were cut with *Nde*I and *Eco*RI and subcloned into the respective sites of expression vector pLZZH13 [9] to yield plasmids pLZ01 and pLZZG07, which harbored wild-type $phaG_{Pp}$ and $phaG_{Pm}$, respectively (Table 1).

2.4. Cellular dry weight and PHA analysis

To determine the cellular dry weight (CDW), liquid cultures were centrifuged at 8000*g* for 15 min, followed by washing twice with saline and 24 h lyophilization. Gas chromatography (GC) analysis of intracellular PHA content and PHA composition were performed as described previously (Hewlett-Packard model 6890 plus, HP, USA) [18]. Relative PHA content was considered as a reference of PhaG in vivo activity.

Downloaded from http://femsle.oxfordjournals.org/ by guest on January 23, 2016

Table 1
Bacterial strains, plasmids and oligonucleotides used in this study

Stains and plasmids	Relevant characteristic(s)*	Source or reference
Strains		
Burkholderia caryphylli AS 1.2741	Wild-type; rRNA homology group II	[9]
Escherichia coli S17-1	*recA*; harbors the *tra* genes of plasmid RP4 in the chromosome; *proA thi*-1	[16]
XL10-Gold	*Tet(r)*; Δ *(mcrA)183* Δ *(mcrCB-hsdSMR-mrr)173 endA1 sup E44 thi-1 recA1 gyrA96 relA1 lac Hte* [F′ *proAB* $lacI^q$ *Z* Δ *M15* Tn10(*tet(r)*) *Amy Cam(r)*]	Stratagene Co.
Pseudomonas mendocina LZ	Wild-type; rRNA homology group I, non-fluorescent pigment produced	This study
Pseudomonas nitroreducens 0802	Wild-type; natural relationship is tentative, fluorescent pigment produced	[9]
Pseudomonas putida $PHAG_N$-21	PhaG-negative mutant of *P. putida* KT2440	[10]
Pseudomonas stutzeri 1317	Wild-type; rRNA homology group I, non-fluorescent pigment produced	[9]
Plasmids		
pGEM®-T	*Ap(r)*; *lacPOZ′*; T-vector	Promega Co.
pLZZH13	pBBR1MSC-2 containing *R. eutropha* PHB-synthesis-locus's promoter with a *Nde* I site at the exactly translate start point	[9]
pLZZGPp	*Ap(r)*; containing *phaG* gene from *P. putida*	[11]
pLZ01	pLZZH13 containing wild-type $phaG_{Pp}$ gene	This study
pLZ02	pLZZH13 containing S78C mutant $phaG_{Pp}$ gene	This study
pLZ03	pLZZH13 containing C78S mutant $phaG_{Pm}$ gene	This study
pLZ04	pLZZH13 containing C78T mutant $phaG_{Pm}$ gene	This study
pLZ05	pLZZH13 containing mutant $phaG_{Pp}$ gene with L110 deletion	This study
pLZ06	pLZZH13 containing mutant $phaG_{Pp}$ gene with A111 deletion	This study
pLZ07	pLZZH13 containing mutant $phaG_{Pp}$ gene with L112 deletion	This study
pLZ08	pLZZH13 containing mutant $phaG_{Pp}$ gene with A111/L112 deletion	This study
pLZ09	pLZZH13 containing mutant $phaG_{Pm}$ gene with A111/L112 insertion	This study
pLZZG07	pLZZH13 containing wild-type $phaG_{Pm}$ gene	This study
Oligonucleotides	DNA sequence	
For amplification of phaG genes		
NT	5′-CCCCAACATATGAGGCCAGAAAT-3′	
CT	5′-ACCCAGGAATTCAGATGGCAAAT-3′	
For RT-PCR		
RN	5′-CGGCCGAAAACACGATCATCC-3′	
RC	5′-TTCACGCACGGTTGGCTTGAG-3′	
For site-specific mutagenesis		
S78C	5′-GGAACGGCTGATC*TGC*AAGGAGACCGAGG-3′	
C78S	5′-GGAACGGCTGATC*AGC*AAGGAGACCGAGG-3′	
C78T	5′-GGAACGGCTGATC*ACC*AAGGAGACCGAGG-3′	
For deletion		
d A111	5′-GCAAGCACGCTGCTG~~GCG~~CTGGCGCACCAGCCG-3′	
d L110	5′-GGCGCAAGCACGCTG~~CTG~~GCGCTGGCGCACCAG-3′	
d L112	5′-GCACGCTGCTGGCG~~CTG~~GCGCACCAGCCGCGG-3′	
dLA	5′-GGCGCAAGCACGCTG~~CTGGCG~~CTGGCGCACCAGCCG-3′	
For insertion		
INS	5’-GGCGCAAGCACGCTGCTGGCGCTGGCGCACCAGCCG-3’	

Restriction endonuclease digestion sites are underlined; site-specific mutation sites are italicised; deletions are scored through; insertions are boxed.
* *Ap(r)*, ampicillin resistant gene; *Kn(r)*, kanamycin resistant gene; gene *phaG* encodes (*R*)-3-hydroxydecanoyl-ACP:CoA transacylase.

2.5. Reverse transcriptase-coupled polymerase chain reaction (RT-PCR) analysis of phaG gene expression

Using commercial kits (Shenergy Biocolor Biol. Sci. & Technol. Co., Shanghai, China), total RNA was isolated and purified from bacterial cultures after 24 h cultivation in MS medium containing 20 g L^{-1} sodium gluconate and 50 mg L^{-1} kanamycin. Purified total RNA was quantified using a UV/Vis Spectrophotometer (Ultraspec 3300, Biochrom, USA). One microgram total RNA was reverse transcribed into cDNA in a 10-μl reaction mixture of the cDNA Cycle Kit (Invitrogen, USA). Then an amount of reverse transcriptase reaction product (2.5 μl for wild-type strains; 1 μl for recombinants) was used as template for PCR amplification. RT-PCRs were performed with primers RN and RC (25 pmol each; Table 1) and 2.5 U *Ex Taq* DNA polymerase in a Mastercycler Grandient Autorisierter Thermocycler (Eppendorf, Germany) for 20 cycles. RT-PCR products were separated on a 1.5% agarose gel and stained with ethidium bromide to investigate the transcription of *phaG* genes. DNA Marker DL 2000 (TaKaRa, Dalian, China) was used as standard.

Downloaded from http://femsle.oxfordjournals.org/ by guest on January 23, 2016

2.6. Statistical analysis

Data are presented as means ± standard errors of the mean (SEM) of four parallel samples. Statistical comparisons were performed using the one-way ANOVA and Student *t*-test with SPSS software (SPSS, Germany). P values < 0.01 were considered statistically significant.

3. Results

3.1. Cloning the phaG gene from P. mendocina LZ

Newly isolated strain *P. mendocina* LZ was designated as a mcl-PHA producing bacteria because it can accumulate 19.4% mcl-PHA (mol%: 3HHx 6.0, 3HO 89.2, 3HD 4.8) on MS medium containing 2 g L^{-1} sodium octanoate after 48 h of cultivation, whereas only negligible PHA (<1%) was produced when unrelated carbon sources, such as 20 g L^{-1} sodium gluconate, were supplied as the sole carbon source. Surprisingly, employing the touchdown PCR method developed previously [9], a distinct PCR product of approximate 900 bp was obtained, in good agreement with the length of the *phaG* gene. Furthermore, DNA sequencing indicated that this DNA fragment exhibited extremely high homology to identified *phaG* genes such as $phaG_{Pp}$ from *P. putida* (Fig. 1(a)). The nucleotide sequence of this amplified DNA fragment, namely $phaG_{Pm}$, will appear in the GenBank database under the Accession No. AY338498.

3.2. Gene $phaG_{Pm}$ expression of natural P. mendocina LZ

Total RNA of *P. mendocina* LZ grown on MS medium containing 20 g L^{-1} sodium gluconate was isolated to investigate *phaG* gene expression by RT-PCR. Employing DNA sequencing as a means of identification, an approximately 760-bp RT-PCR product was recognized as the expression reference of $phaG_{Pm}$. Therefore, unlike *phaG* from *P. nitroreducens* 0802, $phaG_{Pm}$ could be expressed under normal PHA accumulation conditions as well as that of *phaGs* from the typical PHA producing strains *P. stutzeri* 1317 and *B. caryophylli* AS 1.2741 (Fig. 2(a)).

3.3. Mutagenesis of $PhaG_{Pp}$ and $PhaG_{Pm}$

Because heterologous expression of $phaG_{Pm}$ in PhaG-negative mutant *P. putida* $PHAG_N$-21 did not raise in vivo transacylase activity (Table 2), the two sites of amino acid differences between $PhaG_{Pp}$ and $PhaG_{Pm}$ (Fig. 1(b)) were presumed to be essential in maintaining transacylase activity. A mutagenesis assay was employed to test this hypothesis. Firstly, it is worth noting that the mutagenesis in this study did not influence the level of *phaG* gene expression in recombinant *P. putida* $PHAG_N$-21 grown on MS medium containing 20 g L^{-1} sodium gluconate (Fig. 2(b)).

In vivo transacylase activity was still observed in the S78C mutant of $PhaG_{Pp}$ (11.9% PHA accumulation, approximately 51% of wild-type), while no activity was observed in C78S or C78T $PhaG_{Pm}$ mutants as well as

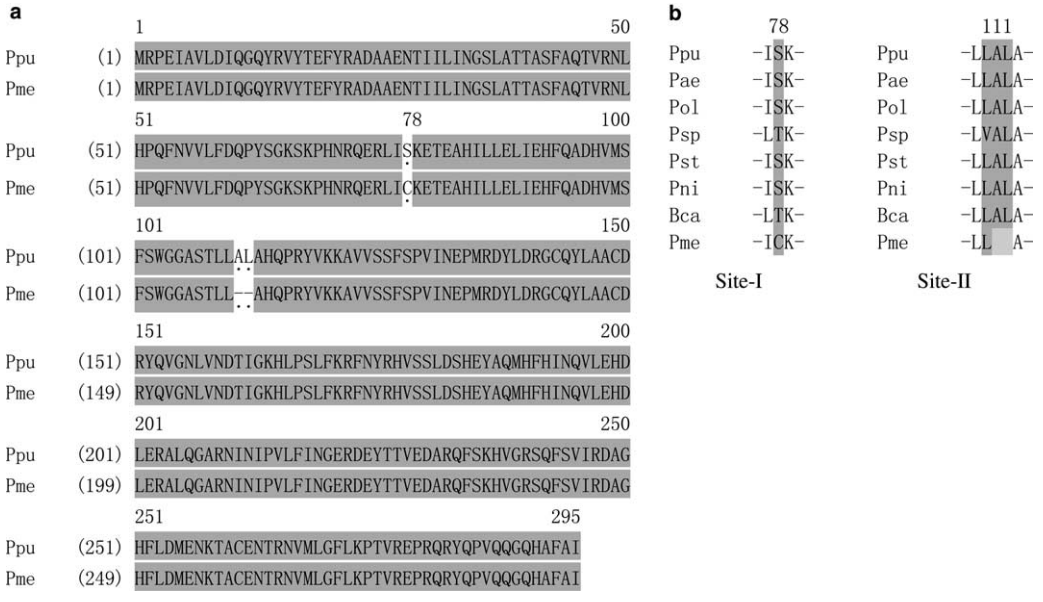

Fig. 1. Alignment of the deduced amino acid sequences of various bacterial *phaG* genes. (a) Whole sequence comparison between PhaG from *P. putida* and from *P. mendocina* LZ. (b) Partial sequence comparison of various bacterial PhaG proteins. Ppu, *P. putida*; Pae, *P. aeruginosa*; Pol, *P. oleovorans*; Psp, *Pseudomonas* sp. 61-3; Pst, *P. stutzeri* 1317; Pni, *P. nitroreducens* 0802; Bca, *B. caryophylli* AS 1.2741; and Pme, *P. mendocina* LZ.

Downloaded from http://femsle.oxfordjournals.org/ by guest on January 23, 2016

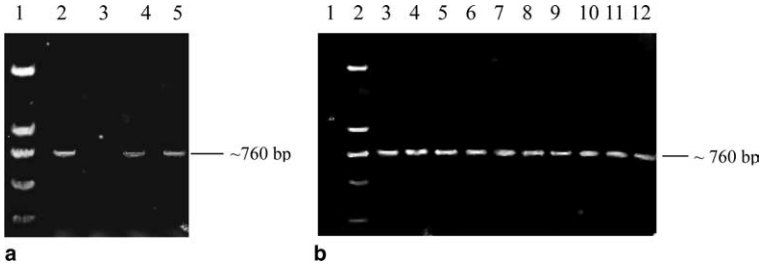

Fig. 2. RT-PCR analysis of *phaG* gene expression in strains grown on MS medium containing 20 g L^{-1} sodium gluconate. (a) Lane 1, DNA Marker DL 2000; lanes 2–5, wild-type strain *B. caryophylli* AS 1.2741, *P. nitroreducens* 0802, *P. mendocina* LZ, and *P. stutzeri* 1317, respectively. (b) Lane 1, recombinant *P. putida* $PHAG_N$-21 harboring plasmid pLZZH13; DNA Marker DL 2,000; lanes 3–12, recombinant *P. putida* $PHAG_N$-21 harboring plasmid pLZ01, pLZZG07, pLZ02, pLZ03, pLZ04, pLZ05, pLZ06, pLZ07, pLZ08, and pLZ09, respectively.

Table 2
PHA accumulation in recombinant *P. putida* $PHAG_N$-21 harboring various *phaG* genes

Plasmid	CDW[b] (g L^{-1})	PHA/CDW (w/w, %)	Composition of PHA (mol %)[a]		
			3HHx	3HO	3HD
pLZZH13	1.08 ± 0.04	1.0 ± 0.1	ND	15.0	85.0
pLZ01	0.97 ± 0.03	21.6 ± 1.1	3.2	40.6	56.2
pLZZG07	1.06 ± 0.01	1.3 ± 0.1	ND	20.8	79.2
pLZ02	0.86 ± 0.02	11.9 ± 0.5	2.7	38.4	58.9
pLZ03	1.02 ± 0.02	1.2 ± 0.1	ND	18.1	81.9
pLZ04	0.93 ± 0.03	1.5 ± 0.3	ND	19.9	80.1
pLZ05	0.89 ± 0.03	1.1 ± 0.2	ND	18.9	81.1
pLZ06	0.74 ± 0.01	0.9 ± 0.1	ND	13.6	86.4
pLZ07	0.81 ± 0.03	1.1 ± 0.2	ND	20.8	79.2
pLZ08	0.85 ± 0.04	1.5 ± 0.2	ND	16.1	83.9
pLZ09	0.86 ± 0.02	11.9 ± 0.5	2.7	38.4	58.9

[a] *P. putida* $PHAG_N$-21 recombinant genes were cultivated on MS medium containing 20 g L^{-1} sodium gluconate and 50 mg L^{-1} kanamycin. After 48 h cultivation at 30 °C and 200 rpm, cells were harvested and analysed. 3HHx, 3-hydroxyhexanoate; 3HO, 3-hydroxyoctanoate; 3HD, 3-hydroxydecanoate; ND, not detectable.
[b] CDW, cellular dry weight.

in the control strain with only 1% PHA accumulation (Table 2). Alternatively, deletion in site II of $PhaG_{Pp}$ led to a dramatic reduction in transacylase activity to approximately 1% PHA accumulation, similar to that of the background (Table 2). Interestingly, insertion of A111 and L112, the two missing amino acid residues at site II (Fig. 1(b)), was able to recover the transacylase activity of $PhaG_{Pm}$, as reflected in an 11.9% PHA accumulation (Table 2).

3.4. Development of PhaG structural model

The conserved domain homology search strongly suggested that $PhaG_{Pp}$ contains an α/β-hydrolase domain. An alignment revealed that the region of amino acid residues 54–261 exhibited 40% similarity and 27.7% identity with the conserved α/β-hydrolase domain (Fig. 3(a)). Reverse Position Specific (RPS)-BLAST (http://www.ncbi.nlm.nih.gov/Structure/cdd/wrpsb.cgi) and 3D-JIGSAW similarity searches [19] resulted in an alignment showing above 30% similarity between $PhaG_{Pp}$ and a typical α/β-hydrolase superfamily protein epoxide hydrolase of *Agrobacterium radiobacter* (1ehy) [20] (Fig. 3(b)). This alignment, in combination with the conserved domain alignment, was used to generate a 3-D structural model of $PhaG_{Pp}$ (Fig. 4(a)) using the 3D-JIGSAW Comparative Modelling Server [19]. The C-terminal region (amino acids 271–295) was deleted in the $PhaG_{Pp}$ used for the protein model. The resulting model suggests that $PhaG_{Pp}$ is a member of the protein family possessing an α/β-hydrolase fold, the core structure, as in the case of the epoxide hydrolase. Inspection of the protein model of $PhaG_{Pp}$ showed that the putative active triad S102-D223-H251 was adjacent to the core structure (Fig. 4(c)). Residue S102 is located at the nucleophile elbow, a sharp γ turn containing the nucleophile residue, positioned between β-strand e5 and α-helix h3 (Figs. 3(b) and 4(c)), which is one of the most conserved features of the α/β-hydrolase enzymes. The model also revealed that S78 was located in a hydrophilic hole on the enzyme surface, which is apart from the catalytic triad. The α-helix h3 and α-helix h10 formed a tunnel towards the active triad, where the groove formed by e8-H251 and h7–h8 located on the other side (Figs. 4(a) and (c)).

A 3-D structural model of the inactive protein $PhaG_{Pm}$ was also constructed by a similar process (Figs. 4(b) and (d)). Compared with the $PhaG_{Pp}$ structural

Downloaded from http://femsle.oxfordjournals.org/ by guest on January 23, 2016

a

```
PhaG   54  FNVVLYDQPYAGKSKAHNLHEKMLTKEIEGQILLELIDHFAAE—HVLSFSWGGAAALVA  111
SIMI       F+V+L+D    GKS   +L E     +   + L  L+D    +  +++  S GG  AL
α/β    1   FDVILFDLRGFGKSSPPDLDE—YRFDDLAEDLEALLDALGLDKVNLVGHSMGGLIALAY   58

PhaG   112 LAHRPRRIKKAVISSFSPVINEPMREYLERGVDYLGNLDRDRVGHLVNNTIGKHLPSLFK  171
SIMI       A  P R+K  V+                        L     +R    V   +G+     F
α/β    59  AAKYPERVKALVLVGPVHPALLSAPLTPRNTPGLLLANFFNRLLRSVEALLGRAPKQFFL  118

PhaG   172 RFNYRHVSTLAEHEY----GQMRFHISDVLNSDRFCYL------NAAKKIDIPVLFMNGE  221
SIMI              L +               D L       L       A K+ID+P L + G
α/β    119 LGRPFVGDFLKQFELSSLIRFGETDGGDGLLGALLGKLLQWDLSAALKRIDVPTLVIWFT  178

PhaG   222 WDEYTAADDARIFADHVQHSTFSIIQAAGHFLDMEHKAAC    261
SIMI       D     D +   A    ++    I  AGH   +E
α/β    179 DDPLVPPDASEKLAALFPNAQVVVIPDAGHLAQLEKPDEV    218
```

b

```
          1                                                          60
SS-q      ---CCCCCEE EEEC-CCCEE EEEEECCCCC CCEEEEECCC CCCHHHHHHH HHHHHCCCEE
PhaG      ---MRPEIAV LDIQ-GQYRV YTEFYRADAA ENTIILINGS LATTASFAQT VRNLHPQFNV
SIMI            +     ++Q     ++         ++A   T++L+ G   +    ++   +  L   + V
1ehy      AIRRPEDFKH YEVQLPDVKI HY---VREGA GPTLLLLHGW PGFWWEWSKV IGPLAEHYDV
SS-m      CCCCHHHCCE EEEECCCCEE EE---EEEEC CCEEEEECCC CCCHHHHHHH HHHHHCCCEE
ACCI      *334276164 4627197131 11---13256 6511111111 1111111121 1341284111
                    e1          e2          e3              h1
          61                                                         120
SS-q      EEECCCCCCCC CCCCCCCC-C CCCHHHHHHH HHHHHHHCCC --EEEEEECH HHHHHHHHHH
PhaG      VLFDQPYSGK SKPHNRQE-R LISKETEAHI LLELIEHFQA --DHVMSFSW GGASTLLALA
SIMI      ++ D    G  S       +     S +  A    + L++         V    + ++      +
1ehy      IVPDLRGFGD SEKPDLNDLS KYSLDKAADD QAALLDALGI EKAYVVGHDF AAIVLHKFIR
SS-m      EEECCCCCCC CCCCCCCCHH HHCHHHHHHH HHHHHHHCCC CCEEEEEECH HHHHHHHHHH
ACCI      1111111113 1421628336 4121331121 1121166281 7611111111 1121111111
          e4                              h2              e5          h3
          121                                                        180
SS-q      HHHHHHHEEE EECCC-CCCC CCHHHHHHHH HHH-HHCCCH HHHHHHHHHH HHH---CCHH
PhaG      HQPRYVKKAV VSSFS-PVIN EPMRDYLDRG CQY-LAACDR YQVGNLVNDT IGK---HLPS
SIMI           V DA+ +     P          +          +++  R
1ehy      KYSDRVIKAA IFDPIQPDFE SWYSQFHQLD MAVEVVGSSR EVCKKYFKHF FDHWSYRDEL
SS-m      HCHHHEEEEE EECCCCCCCC CHHHHHCCCH HHHHHHCCCH HHHHHHHHHH HHHCCCCCCC
ACCI      5267113311 1112312456 1111311326 1125114434 5113311321 1241154961
             h4      e6           h5          h6           h7
          181                                                        240
SS-q      HHHHHHHHHH HHCCCCCHHH HHHHHHHHHH CCCCCHHHHH --HCCCCCEE EEECCCCCCC
PhaG      LLKRFNYRHV SSLDSHEYAQ MHFHINQVLE HDLERALQGA --RNINIPVL FINGERDEYT
SIMI      L       HV          +    F    +        +   +       +PVL  I G  D
1ehy      LTEEELEVHV DNCMKPDNIH GGFNYYRANI RPDAALWTDL DHTMSDLPVT MIWGLGDTCV
SS-m      CCHHHHHHHH HHHCCCCHHH HHHHHHHHHC CCCCCCCCCH HHCCCCCCEE EEEECCCCCC
ACCI      2564113111 5113486112 1111111212 3632424254 1445172312 1111223654
               h8              h9                          e7
          241                                        285
SS-q      CHHHHHHHH- HHCCCCEEEE ECCCCCCHHH CCHHHHHHHH HHHHH
PhaG      TVEDARQFS- KHVGRSQFSV IRDAGHFLDM ENKTACENTR SVMLG
SIMI         +  F   K          I D GHFL   E   +
1ehy      PYAPLIEFVP KYYSNYTMET IEDCGHFLMV EKPEIAIDRI KTAFR
SS-m      5125245415 5215535344 1851111111 1326312531 46219
ACCI      CCHHHHHHHH HHCCCEEEEE ECCCCCCHHH HCHHHHHHHH HHHCC
          h10             e8                    h11
```

Fig. 3. (a) Alignment of $PhaG_{Pp}$ with the conserved α/β-hydrolase fold region. The alignment was performed using the RPS-BLAST search. PhaG, amino acid sequence of $PhaG_{Pp}$; SIMI, showing similarity (+) and amino acids in the proteins that are identical in that position; α/β, α/β-hydrolase fold region. (b) Alignment of the $PhaG_{Pp}$ with epoxide hydrolase from *A. radiobacter* (1ehy). The alignment was performed using the 3D-JIGSAW Comparative Modelling Server. SS-q, predicted secondary structure of query ($PhaG_{Pp}$); PhaG, amino acid sequence of $PhaG_{Pp}$; SIMI, showing similarity (+) and amino acids in the proteins that are identical in that position; 1ehy, amino acid sequences of epoxide hydrolase from *A. radiobacter*; SS-m, known secondary structure of template (epoxide hydrolase from *A. radiobacter*); ACCI, relative solvent accessibility for each residue of the template. Predicted secondary structures of $PhaG_{Pp}$ are shaded.

Downloaded from http://femsle.oxfordjournals.org/ by guest on January 23, 2016

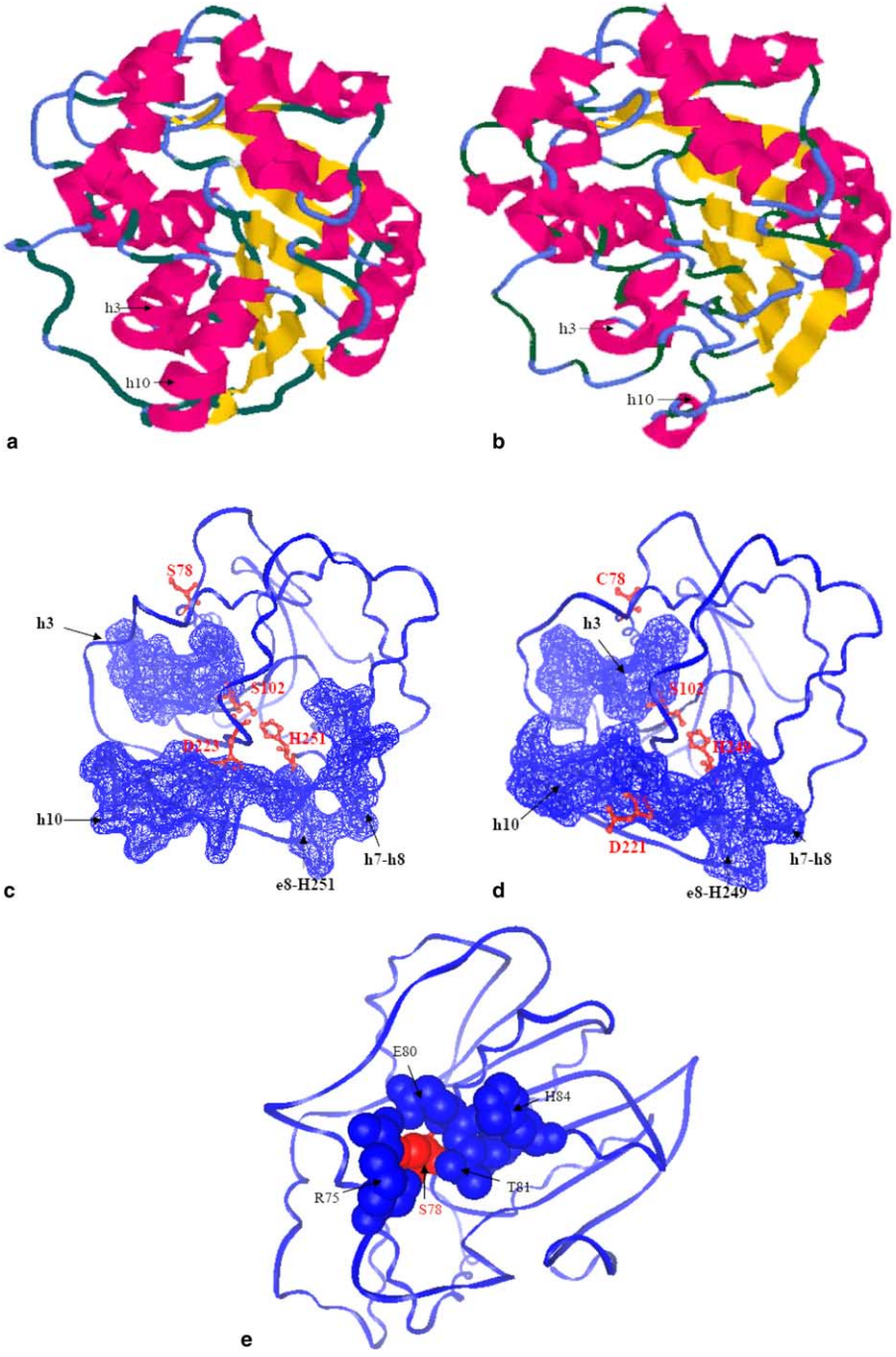

Fig. 4. 3-D structural models of $PhaG_{Pp}$ and $PhaG_{Pm}$ performed by the 3D-JIGSAW server. (a), (c) and (e), $PhaG_{Pp}$; (b) and (d), $PhaG_{Pm}$. (a) and (b) show the predicted secondary structures; (c) and (d) show the putative active triad S102-D223/221-H251/249 and their environments; (e) shows the position of S78 and its environment in $PhaG_{Pp}$.

model, substitution at position 78 (site I, Fig. 1(b)) did not alter the protein structure (Fig. 4). However, the disruption of amino acid sequences in the region 109–111 (site II, Fig. 1(b)) corresponding to α-helix h3 led to a significant structural distortion (Figs. 1, 3(b) and Fig. 4), reflected in the shortening of α-helix h3 (Figs. 4(a) and (b)), and the disappearance of the groove formed by e8-H251/H249 and h7–h8 (Figs. 4(c) and (d)). At the same time, α-helix h10 was completely destroyed, and then one of the active sites D223/D221 was exposed to the protein surface (Figs. 4(b) and (d)).

4. Discussion

PHA metabolism has been intensely investigated in many bacteria. Genes and proteins involved in PHA synthesis have been cloned and analyzed [1–3]. Fatty acid

Downloaded from http://femsle.oxfordjournals.org/ by guest on January 23, 2016

metabolic pathways have been reported to be the most common routes to supply the precursors for PHA synthesis [21], especially in *Pseudomonas* strains [22]. Employing (*R*)-specific enoyl-CoA hydratase, degradation of alkanoates via β-oxidation can provide various intermediates for mcl-PHA synthesis [23]. The fatty acid de novo biosynthesis pathway can also provide mcl-PHA precursors from carbon sources unrelated to PHA monomer structure by mobilizing 3-ketoacyl-ACP reductase [24] or PhaG [10]. Recent studies have shown that the PhaG-mediated mcl-PHA biosynthesis pathway occurs in a broad range of bacterial species [9,10,13–15]. The pathway appears to play an important function during evolution. Both RPS-BLAST (Fig. 3(a)) and 3-D structure prediction (Fig. 4(a)) strongly suggest that PhaG belongs to the α/β-hydrolase superfamily with its active sites situated on S102, D223 and H251 [25]. The metabolic mechanism of PhaG-catalyzed acyl transaction has been studied by site-specific mutations [25,26] which implied that the HX_4D motif found in most transacylases did not present a specific function to PhaG. These studies suggested that this new family of transacylase, which catalyzed in vivo conversion from (*R*)-3-hydroxyacyl-ACP to CoA thioester, exerted a reaction mechanism similar to that of serine hydrolases and acyl transferases [25]. Because the 3-D structure of PhaG has not yet been resolved, native inactive PhaG protein not being available, previous studies were only focused on the catalytic active center. Further details of PhaG are still under investigation.

A newly isolated strain which belongs to rRNA homologous group I containing γ subdivision Proteobacteria, termed *P. mendocina* LZ, could accumulate mcl-PHA from related carbon sources, such as octanoate, instead of unrelated carbon sources, such as gluconate. This indicated that this strain harbours a functional PHA synthase system, but the precursor metabolic pathway from unrelated carbon sources might be absent or blocked. Interestingly, a DNA fragment with high homology to reported *phaG* genes, namely $phaG_{Pm}$, was cloned from this strain. Furthermore, RT-PCR analysis showed that the $phaG_{Pm}$ gene was transcribed in the wild-type bacterium when carbohydrates were supplied as the sole carbon sources (Fig. 2(a)). Thus, the absent ability of mcl-PHA synthesis from unrelated carbon sources could be contributed to neither the absence of an enzyme coupled carbohydrate metabolism and PHA precursor supplement as in the case of *P. fragi* [27], nor the inefficient transcription of the *phaG* gene as in the cases of *P. oleovorans* [14] and *P. nitroreducens* 0802 (Fig. 2(a), and [9]). At the same time, introduction of $phaG_{Pm}$ into the reported successful *phaG*-gene-identification system [9] did not induce intracellular mcl-PHA accumulation. These phenomena provided further evidence that the blocking of the mcl-PHA synthesis pathway from unrelated carbon sources in *P. mendocina* LZ is due to the intrinsic properties of the $PhaG_{Pm}$, encoded by the $phaG_{Pm}$ gene. Hence, $phaG_{Pm}$ can be considered as the first gene encoding a native inactive PhaG protein.

The alignment revealed that this inactive protein exhibited two sites of difference to known active PhaG proteins: cysteine replaced serine or threonine at position 78 of PhaG, and a leucine and an alanine were missing in the region 109–113 (Fig. 1(b)). Furthermore, about 50% in vivo activity was observed in mutated $PhaG_{Pp}$ S78C (Table 2). Comparing the 3-D structural models of PhaGs developed in this study (Fig. 4(c) and (d)), it is quite possible that the side-chain hydroxyl group of the 78th amino acid residue plays a supporting role in exerting the PhaG function. Considering its hydrophilic environment and the concave location, this position is more likely to be a post-translational modification site rather than a protein–protein interaction site (Fig. 4(e)). On the other hand, site II (region 109–113) was more important for maintaining PhaG activity (Table 2), though it was not enclosed in the active center of the enzyme (Fig. 4). This region was assembled into a hydrophobic α-helix h3 (Fig. 3(a)); it provided a hydrophobic environment surrounding the catalytic triad, together with other surrounding fragments such as α-helix h10 (Figs. 4(a) and (c)). Alteration on region h3 not only changed its own structure but also destroyed contiguous fragments including the h10 helix, resulting in increasing stress within the protein structure (Fig. 4(b)). Thus, the catalytic triad disassembled following the exposure of D223/D221 to the protein surface and the disappearance of the proximate groove (Fig. 4(d)). The above variations reduced the accessibility of the protein active sites, resulting in complete loss of enzyme activity (Table 2). These results demonstrated that the surrounding region of the active center can significantly influence the enzyme activity. These amino acid fragments should not be ignored during protein engineering for enhanced activity and reduction in substrate specificity.

In summary, for the first time, in this study, we cloned an inactive PhaG-encoding gene from *P. mendocina* LZ and elucidated the reason why the protein lost its function. Our result supports the hypothesis that PhaG contains a S102-D223-H251 (for PhaG from *P. putida*) catalytic triad instead of the normal HX_4D transacylase motif [25,26]. More importantly, this is the first report to describe the loss of PhaG activity due to the disruption of its non-active center region. This study will be helpful for further understanding of the PhaG protein. It also suggests that there may be various molecular methods for protein molecular evolution.

Acknowledgments

The authors acknowledge Professor A. Steinbüchel of the Westfälische Wilhelms-Universität Münster in Germany for his kind donation of *P. putida* $PHAG_N$-21

Downloaded from http://femsle.oxfordjournals.org/ by guest on January 23, 2016

and *phaG* gene of *P. putida*. This research was supported by the Natural Sciences Foundation of China Grant Nos. 30170017 and 20334020. The State 863 funds also provided financial contribution to this study.

References

[1] Anderson, A.J. and Dawes, E.A. (1990) Occurrence, metabolism, metabolic role and industrial uses of bacterial polyhydroxyalkanoates. Microbiol. Rev. 54, 450–472.
[2] Madison, L.L. and Huisman, G.W. (1999) Metabolic engineering of poly(3-hydroxyalkanoates): from DNA to plastic. Microbiol. Mol. Biol. Rev. 63, 21–53.
[3] Steinbüchel, A. and Lütke-Eversloh, T. (2003) Metabolic engineering and pathway construction for biotechnology production of relevant polyhydroxyalkanoates in microorganisms. Biochem. Eng. J. 16, 81–96.
[4] Jendrossek, D., Schirmer, A. and Schleger, H.G. (1996) Biodegradation of polyhydroxyalkanoaoic acids. Appl. Microbiol. Biotechnol. 46, 451–463.
[5] Chen, G.Q. and Wu, Q. (2005) Polyhydroxyalkanoates as tissue engineering materials. Biomaterials 26, 6565–6578.
[6] Zheng, Z., Deng, Y., Lin, X.S., Zhang, L.X. and Chen, G.Q. (2003) Induced production of rabbit articular cartilage-derived chondrocytes collagen II on polyhydroxyalkanoates blends. J. Biomater. Sci. Polym. Ed. 14, 615–624.
[7] Zheng, Z., Bei, F.F., Tian, H.L. and Chen, G.Q. (2005) Effects of crystallization of polyhydroxyalkanoate blend on surface physiochemical properties and interactions with rabbit articular cartilage chondrocytes. Biomaterials 26, 3537–3548.
[8] Huisman, G.W., de Leeuw, O., Eggink, G. and Witholt, B. (1989) Synthesis of poly-3-hydroxyalkanoates is a common feature of fluorescent pseudomonads. Appl. Environ. Microbiol. 55, 1949–1954.
[9] Zheng, Z., Chen, J.C., Tian, H.L., Bei, F.F. and Chen, G.-Q. (2005) Specific identification of (*R*)-3-hydroxyacyl-ACP:CoA transacylase gene from *Pseudomonas* and *Burkholderia* strains by polymerase chain reaction. Chin. J. Biotechnol. 21, 19–24.
[10] Rehm, B.H.A., Krüger, N. and Steinbüchel, A. (1998) A new metabolic link between fatty acid *de novo* synthesis and polyhydroxyalkanoic acid synthesis. J. Biol. Chem. 273, 24044–24051.
[11] Zheng, Z., Zhang, M.J., Zhang, G. and Chen, G.Q. (2004) Production of 3-hydroxydecanoic acid by recombinant *Escherichia coli* HB101 harboring *phaG* gene. Antonie van Leeuwenhoek 85, 93–101.
[12] Zheng, Z., Gong, Q., Liu, T., Deng, Y., Chen, J.C. and Chen, G.Q. (2004) Thioesterase II of *Escherichia coli* plays an important role in 3-hydroxydecaoic acid production. Appl. Environ. Microbiol. 70, 3807–3813.
[13] Hoffmann, N., Steinbüchel, A. and Rehm, B.H.A. (2000) The *Pseudomonas aeruginosa phaG* gene product is involved in the synthesis of polyhydroxyalkanoic acid consisting of medium-chain-length constituents from non-related carbon sources. FEMS Microbiol. Lett. 184, 253–259.
[14] Hoffmann, N., Steinbüchel, A. and Rehm, B.H.A. (2000) Homologous functional expression of cryptic *phaG* from *Pseudomonas oleovorans* establishes the transacylase-mediated polyhydroxyalkanoate biosynthetic pathway. Appl. Microbiol. Biotechnol. 54, 665–670.
[15] Matsumoto, K., Matsusaki, H., Taguchi, S., Seki, M. and Doi, Y. (2001) Cloning and characterization of *Pseudomonas* sp. 61-3 *phaG* gene involved in polyhydroxyalkanoate biosynthesis. Biomacromolecules 2, 142–147.
[16] Simon, R., Priefer, U. and Pühler, A. (1983) A broad host range mobilization system for *in vivo* genetic engineering: transposon mutagenesis in Gram-negative bacteria. Bio/Technology 1, 784–791.
[17] Sambrook, J. and Russel, D.W. (2001) Molecular Cloning: A Laboratory Manual, third ed. Cold Spring Harbor Laboratory, Cold Spring Harbor, NY.
[18] Hang, X.M., Lin, Z.X., Chen, J.Y., Wang, G.L., Hong, K. and Chen, G.Q. (2002) Polyhydroxyalkanoate biosynthesis in *Pseudomonas pseudoalcaligenes* YS1. FEMS Microbiol. Lett. 212, 71–75.
[19] Bates, P.A., Kelley, L.A., MacCallum, R.M. and Stenberg, M.J.E. (2001) Enhancement of protein modeling by human intervention in applying the automatic program 3D-JIGSAW and 3D-PSSM. Proteins: Struct. Funct. Genet. 5 (Suppl.), 39–46.
[20] Nardini, M., Ridder, I.S., Rozeboom, H.J., Kalk, K.H., Rink, R., Janssen, D.B. and Dijkstra, B.W. (1999) The X-ray structure of epoxide hydrolase from *Agrobacterium radiobacter* AD1. An enzyme to detoxify harmful epoxides. J. Biol. Chem. 274, 14579–14586.
[21] Sudesh, K., Abe, H. and Doi, Y. (2000) Synthesis, structure and properties of polyhydroxyalkanaotes: biological polyesters. Prog. Polym. Sci. 25, 1503–1555.
[22] Huijbert, G.N.M., de Rijk, T.C., de Waard, P. and Eggink, G. (1994) ^{13}C nulear magnetic resonance studies of *Pseudomonas putida* fatty acid metabolic routes involved in poly(3-hydroxyalkanoates) synthesis. J. Bacteriol. 176, 1661–1666.
[23] Tsuge, T., Fukui, T., Matsusaki, H., Taguchi, S., Kobayashi, G., Ishizaki, A. and Doi, Y. (1999) Molecular cloning of two (*R*)-specific enoyl-CoA hydratase genes from *P. aeruginosa* and their use for polyhydroxyalkanoate synthesis. FEMS Microbiol. Lett. 184, 193–198.
[24] Ren, Q., Sierro, N., Witholt, B. and Kessler, B. (2000) FabG, an NADPH-dependent 3-ketoacyl reductase of *Pseudomonas aeruginosa*, provides precursors for medium-chain-length poly-3-hydroxyalkanoate biosynthesis in *Escherichia coli*. J. Bacteriol. 182, 2798–2981.
[25] Hoffman, N., Amara, A.A., Beermann, B.B., Qi, Q., Hinz, H.J. and Rehm, B.H.A. (2002) Biochemical characterization of the *Pseudomonas putida* 3-hydroxyacyl ACP:CoA transacylase, which diverts intermediates of fatty acid *de novo* biosynthesis. J. Biol. Chem. 277, 42926–42936.
[26] Matsumoto, K., Matsusaki, H., Taguchi, S., Seki, M. and Doi, Y. (2001) Cloning and characterization of the *Pseudomonas* sp. 61-3 *phaG* gene involved in polyhydroxyalkanoate biosynthesis. Biomacromolecules 2, 142–147.
[27] Fiedler, S., Steinbüchel, A. and Rehm, B.H. (2002) PhaG-mediated synthesis of poly(3-hydroxyalkanoates) consisting of medium-chain-length constituents from nonrelated carbon sources in recombinant *Pseudomonas fragi*. Appl. Environ. Microbiol. 66, 2117–2124.

Downloaded from http://femsle.oxfordjournals.org/ by guest on January 23, 2016